Coupled Systems Mechanics, *Vol. 10, No. 5 (2021) 393-414*
https://doi.org/10.12989/csm.2021.10.5.393

Hyperstatic steel structure strengthened with prestressed carbon/glass hybrid laminated plate

Hassaine Daouadji Tahar*[1,2], Rabahi Abderezak[1,2] and Benferhat Rabia[1,2]

[1]*Civil Engineering Department, University of Tiaret, Algeria*
[2]*Laboratory of Geomatics and Sustainable Development, University of Tiaret, Algeria*

(Received June 8, 2021, Revised July 8, 2021, Accepted July 9, 2021)

Abstract. This paper presents a careful theoretical investigation into interfacial shear stresses in steel beam strengthened with prestressed carbon/glass hybrid laminated plate. A closed-form rigorous solution for interfacial shear stress in steel beams strengthened with bonded prestressed carbon/glass hybrid laminated plates and subjected to a uniformly distributed load, is developed using linear elastic theory and including the variation in fiber volume fraction of carbon/glass hybrid laminated. The results show that there exists a high concentration of shear stress at the ends of the laminate, which might result in premature failure of the strengthening scheme at these locations. A parametric study has been conducted to investigate the sensitivity of interface behavior to parameters such as laminate and adhesive stiffness, the proportions and volume fraction of the fiber of carbon/glass hybrid laminated, the thickness of the laminate and the effect of prestressing where all were found to have a marked effect on the magnitude of maximum shear and normal stress in the composite member. This solution is intended for application to beams made of all kinds of materials bonded with a thin composite plate. This research is helpful for the understanding on mechanical behaviour of the interface and design of such structures.

Keywords: carbon/glass hybrid laminated; prestressed plate; shear stresses; steel beam; strengthening

1. Introduction

As a nation's infrastructure ages, one of the major challenges the construction industry faces is that the number of deficient structures continues to grow. The applications of using externally bonded fiber reinforced polymer laminates to reinforced steel structures have shown that the technique is sound and efficient and offers a practical solution to this pressing problem. Retrofitting using externally bonded plates is quick, easy with respect to material handling, causes minimal site disruption and produces only a small change in section size (Smith and Teng 2002, Tounsi 2006, Hassaine Daouadji *et al*. 2021a). Central to the success of this technique is the effective stress transfer from the existing steel beam to the externally bonded FRP reinforcement. Research has shown that the controlling failure mode of such a strengthened beam often involves premature debonding of the composite plate from the steel beam in a brittle manner (Abderezak *et al*. 2019, Akbas Seref 2018, Hassaine Daouadji *et al*. 2021c, Babak Safaei 2020, Oguzhan Das *et al* 2020, Kadir Mercan *et al* .2020, Ameur *et al*. 2008, Amara *et al*. 2019, Benachour *et al*. 2008, Benferhat

*Corresponding author, Professor, E-mail: daouadjitahar@gmail.com, tahar.daouadji@univ-tiaret.dz

http://www.techno-press.org/?journal=csm&subpage=8 ISSN: 2234-2184 (Print), 2234-2192 (Online)

et al. 2019, Bensattalah *et al*.2020, Benferhat *et al*. 2020a, Rabahi *et al*. 2021c, Bouakaz *et al*. 2014, Hassaine Daouadji 2017, Benferhat *et al*. 2021b, David *et al*. 2020 and Tounsi *et al*. 2008). As this debonding failure mode is closely related to interfacial shear stresses between the composite plate and the existing beam, extensive studies have been carried out during the last decade on the prediction of interfacial shear stress.

The most common failure mode for FRP-strengthened beams is debonding of the composite plate. This premature mode is caused by interfacial stress concentration in the adhesive layer. In recent applications (Hassaine Daouadji *et al*. 2019, Abdelhak *et al*. 2021, Bensatallah *et al*. 2020b, Benhenni *et al*. 2021, Bekki *et al*. 2021, Chergui *et al*. 2019, Chaded *et al*. 2018, Hamrat *et al*. 2020, Kablia *et al*. 2020, Hassaine Daouadji 2013, Rabahi *et al*. 2021a, Benferhat *et al*. 2021c, Rabahi *et al*. 2021d, Tlidji *et al*. 2021, Krour *et al*. 2014, Benferhat *et al*. 2021a, Liu *et al*. 2019; Hassaine Daouadji *et al*. 2021b, Rabahi *et al*. 2021b and Panjehpour *et al*. 2014), prestressing of the composite plates has been employed to increase the efficiency of the strengthening technique and in order to better utilize the ultra high strength of these materials. In the literature, we have found that there is not much study of the concentration of interfacial shear stresses in steel beams reinforced with prestressed laminates (Panjehpour *et al*. 2016, Benferhat *et al*. 2020b, Rabahi *et al*. 2020, Hassaine Daouadji *et al*. 2020, He *et al*. 2019 and AlFurjan 21). To the knowledge of the authors, very few theoretical results that have been published on interfacial shear stress concentration in steel beams reinforced with bonded prestressed laminates considering the current bending load cases. Also we noticed a lack of theoretical results in the literature for the case of hybrid laminated plates. For that we the authors; we thought to present this research, which deals with the case of a steel beam strengthened with prestressed carbon/glass hybrid laminated plate. Closed-form solutions of such stresses are thus required in developing design guidelines for strengthening steel beams with bonded prestressing hybrid laminated plates.

In this paper, a general new solution is developed to predict interfacial shear stress in steel beam strengthened with prestressed carbon/glass hybrid laminated plate subjected to a uniformly distributed load. Hence, compared with the existing solutions such as presented by Hassaine Daouadji (2019), He Model (2019). The present model is general in nature, and it is applicable to more general loads cases. With the escalating use of this strengthening scheme, there is a great need for calculation models that can be used to predict the magnitude of maximum interfacial shear stress at the end of the laminate. There is also some lack of knowledge today regarding how material and geometric properties of the strengthening system (composite materials and adhesive) should be chosen in order to minimize the magnitude of these interfacial stresses and ensure sufficient strength of the strengthening system without need for expensive and complicated mechanical anchorage devices.

2. Analytical solutions of interfacial stresses

2.1 Basic assumptions

The present analysis takes into consideration the transverse shear stress and strain in the continuous steel beam strengthened with prestressed carbon/glass hybrid laminated plate but ignores the transverse normal stress in them. One of the analytical approach proposed by Hassaine Daouadji (2019) for steel beam strengthened with a bonded composite plate (Fig. 1) was used in order to compare it with other analytical solutions.

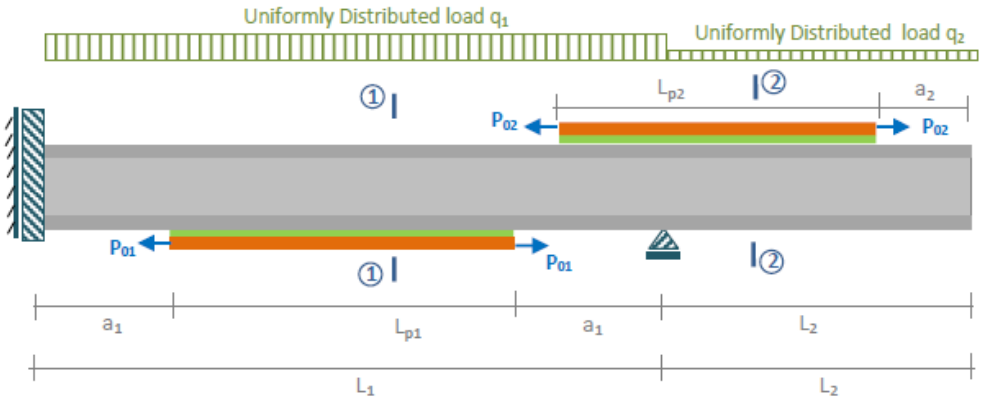

Fig. 1 Steel beam strengthened with prestressed carbon/glass hybrid laminated plate

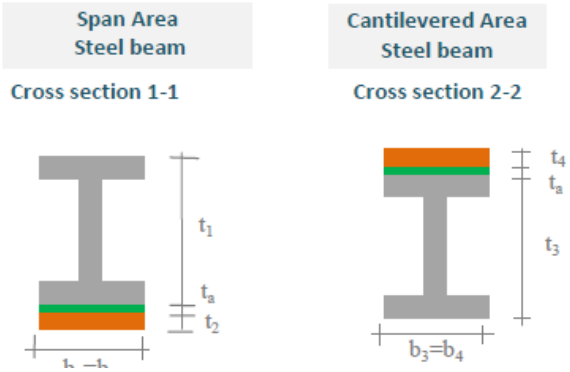

Fig. 2 Steel beam strengthened with prestressed carbon/glass hybrid laminated plate: cross section in span and on both supports

The analytical approach is based on the following assumptions (Hassaine Daouadji 2019):
1. All materials considered are linear elastic.
2. The beam is simply supported and shallow, i.e., plane sections remain plane in bending.
3. No slip is allowed at the interface of the bond (i.e., there is a perfect bond at the adhesive steel or carbon/glass hybrid laminated plate interface).
4. The adhesive is assumed to only play a role in transferring the stresses from the continuous steel beam strengthened with prestressed carbon/glass hybrid laminated plate reinforcement;
5. The stresses in the adhesive layer do not change through the direction of the thickness;
6. The shear stress analysis assumes that the curvatures in the beam and carbon/glass hybrid laminated plate are equal (since this allows the shear stress and peel stress equations to be uncoupled). However, this assumption is not made in the normal stress solution, i.e., when the beam is loaded, vertical separation occurs between steel beam and carbon/glass hybrid laminated plate.
7. A parabolic shear deformation distribution, through the depth of both the beam and the bonded carbon/glass hybrid laminated plate is assumed.
8. Bending deformations of the beam and carbon/glass hybrid laminated composite plate are assumed.

2.2 Elastic properties of hybrid lamina

Hybrid laminated composite plates consisting of two different fibers as carbon/glass, glass/aramid and so on are considered in this study. The mechanical properties of these materials depend on fibers and matrix whose quantities in the materials are specified by volume and mass fractions. The effective elastic properties of this kind of lamina are given by the following equations (Vasiliev and Morozov 2001)

$$E_1 = E_f^{(1)} V_f^{(1)} + E_f^{(2)} V_f^{(2)} + E_m V_m \tag{1}$$

where E_1 is the longitudinal effective modulus, $E_f^{(1)}$ and $E_f^{(2)}$ are Young's moduli of the fibers of the first and of the second type, E_m is the matrix Young's modulus, $V_f^{(1)}$ and $V_f^{(2)}$ are volume fractions of the fibers of the first and of the second type and V_m is the matrix volume fraction, so that

$$V_f^{(1)} + V_f^{(2)} + V_m = 1 \tag{2}$$

$$V_f = V_f^{(1)} + V_f^{(2)} \tag{3}$$

where V_f is the total volume fraction of the fibers. And the normalized volume fractions of fibers are defined as

$$w_f^{(1)} = \frac{V_f^{(1)}}{V_f}, w_f^{(2)} = \frac{V_f^{(2)}}{V_f} \tag{4}$$

so that

$$E_1 = V_f \left[E_f^{(1)} w_f^{(1)} + E_f^{(2)} \left(1 - w_f^{(1)} \right) \right] + E_m \left(1 - V_f \right) \tag{5}$$

The in-plane effective Poisson's coefficient of the hybrid laminated composite ν_{12} can be calculated by

$$\nu_{12} = V_f \left[\nu_f^{(1)} w_f^{(1)} + \nu_f^{(2)} \left(1 - w_f^{(1)} \right) \right] + \nu_m \left(1 - V_f \right) \tag{6}$$

where $\nu_f^{(1)}$ and $\nu_f^{(2)}$ are Poisson's coefficients of the fibers of the first and of the second type, ν_m is the matrix Poisson's coefficient.

The shear moduli of the fibers and the matrix are given by

$$G_f^{(1)} = \frac{E_f^{(1)}}{2\left(1+\nu_f^{(1)}\right)}, \tag{7a}$$

$$G_f^{(2)} = \frac{E_f^{(2)}}{2\left(1+\nu_f^{(2)}\right)}, \tag{7b}$$

$$G_m = \frac{E_m}{2(1+\nu_m)} \tag{7c}$$

where $G_f^{(1)}$ and $G_f^{(2)}$ are shear moduli of the fibers of the first and of the second type, G_m is the matrix shear modulus. The total effective modulus of the fibers is given by

$$G_f = G\nu_f^{(1)} w_f + G_f^{(2)}\left(1 - w_f\right) \tag{8}$$

The compressibility moduli of the fibers and the matrix are given by

$$k_f = \frac{E_f^{(1)} w_f}{3\left(1-2\nu_f^{(1)}\right)} + \frac{E_f^{(2)} w_f}{3\left(1-2\nu_f^{(2)}\right)}, \tag{9a}$$

$$k_m = \frac{E_m}{3(1-2\nu_m)} \tag{9b}$$

The lateral compressibility modulus of the fibers and the matrix are given respectively by

$$K_f = k_f + \frac{G_f}{3} \tag{10a}$$

$$K_m = k_m + \frac{G_m}{3} \tag{10b}$$

The effective shear in-plane and out-of-plane moduli of the composite plate are then given by

$$G_{23} = G_m\left(1 + \frac{V_f}{\frac{G_m}{G_f - G_m} + V_m \frac{k_m + 7G_m/3}{2k_m + 8G_m/3}}\right) \tag{11a}$$

$$G_{12} = G_m \frac{G_f(1+V_f) + G_m(1-V_f)}{G_f(1-V_f) + G_m(1+V_f)} \tag{11b}$$

$$G_{13} = G_{12} \tag{11c}$$

The effective lateral compressibility modulus of the hybrid composite plate is given as

$$K_L = K_m + \frac{V_f}{\frac{1}{k_f - k_m + \frac{1}{3}(G_f - G_m)} + \frac{1-V_f}{k_m + \frac{4}{3}G_m}} \tag{12}$$

Finally, the effective transversal Young's modulus of the hybrid composite plate is given as follows

$$E_2 = \frac{2}{\frac{1}{2K_L} + \frac{1}{2G_{23}} \frac{2(\nu_{12})^2}{E_1}} \tag{13}$$

For the classic laminates (hybrid fiber - matrix):

On the other hand, the laminate theory is used to determine the stress and strain of the externally bonded composite plate in order to investigate the whole mechanical performance of the composite strengthened structure. The effective modules of the composite laminate are varied by the orientation of the fibre directions and arrangements of the laminate patterns. The classical laminate theory is used to estimate the strain of the composite plate, i.e.

The fundamental equation of the laminate theory

$$\begin{Bmatrix} \varepsilon^0 \\ k \end{Bmatrix} = \begin{bmatrix} A' & B' \\ C' & D' \end{bmatrix} \begin{Bmatrix} N \\ M \end{Bmatrix} \tag{14}$$

$$\left[A'\right] = [A]^{-1} + [A]^{-1}[B][D^*]^{-1}[B][A]^{-1}$$
$$\left[B'\right] = -[A]^{-1}\left[B\ \right][D^*]^{-1}$$

$$\begin{gathered}\left[C^{'}\right]=\left[B^{'}\right]^{T}\\ \left[D^{'}\right]=[D^{*}]^{-1}\\ [D^{*}]=[D]-[B][A]^{-1}[B]\end{gathered} \tag{15}$$

The terms of the matrices $[A]$,$[B]$ and $[D]$ are written as:

[A]: Extensional matrix: $A_{ij}=\sum_{k=1}^{NN}\bar{Q}_{ij}^{k}((y_2)_k-(y_2)_{k-1})$ (16)

[B]: Extensional -bending coupled matrix: $B_{ij}=\frac{1}{2}\sum_{k=1}^{NN}\bar{Q}_{ij}^{k}((y_2^2)_k-(y_2^2)_{k-1})$ (17)

[D]: Flexural matrix: $D_{ij}=\frac{1}{3}\sum_{k=1}^{NN}\bar{Q}_{ij}^{k}((y_2^3)_k-(y_2^3)_{k-1})$ (18)

The subscript *NN* represents the number of laminate layers of the FRP plate, the transformed stiffness matrix $[\bar{Q}_{ij}]$ varies with the orientation of the fibers of each layer, then $[\bar{Q}_{ij}]$ can be estimated by using the off-axis orthotropic plate theory, where

The transformed stiffness matrix $[\bar{Q}_{ij}]$: $\overline{Q}_{ij}=\begin{bmatrix}\bar{Q}_{11} & \bar{Q}_{12} & 0\\ \bar{Q}_{21} & \bar{Q}_{22} & 0\\ 0 & 0 & \bar{Q}_{33}\end{bmatrix}$ (19)

Where: $m=cos(\theta_j)$ et $n=sin(\theta_j)$

$$\overline{Q}_{11}=Q_{11}m^4+2(Q_{12}+2Q_{33})m^2n^2+Q_{22}n^4 \tag{20a}$$

$$\overline{Q}_{12}=(Q_{11}+Q_{22}-4Q_{33})m^2n^2+Q_{12}(n^4+m^4) \tag{20b}$$

$$\overline{Q}_{22}=Q_{11}n^4+2(Q_{12}+2Q_{33})m^2n^2+Q_{22}m^4 \tag{20c}$$

$$\overline{Q}_{33}=(Q_{11}+Q_{22}-2Q_{12}-2Q_{33})m^2n^2+Q_{33}(n^4+m^4) \tag{20d}$$

And

$$Q_{11}=\frac{E_1}{1-\upsilon_{12}\upsilon_{21}} \tag{21a}$$

$$Q_{22}=\frac{E_2}{1-\upsilon_{12}\upsilon_{21}} \tag{21b}$$

$$Q_{12}=\frac{\upsilon_{12}E_2}{1-\upsilon_{12}\upsilon_{21}}=\frac{\upsilon_{21}E_1}{1-\upsilon_{12}\upsilon_{21}} \tag{21c}$$

$$Q_{33}=G_{12} \tag{21d}$$

Where j is number of the layer; h, $\bar{Q}_{ij}$ and θ_j are respectively the thickness, the Hooke's elastic tensor and the fibers orientation of each layer.

2.3 Interfacial shear stress distribution along the carbon/glass hybrid laminated -steel interface "Strengthened in Span: lower part"

A differential section dx, can be cutout from the carbon/glass hybrid laminated composite-strengthened steel, as shown in Fig. 3 "*Strengthened in Span: lower part*". The strains in the continuous steel beam near the adhesive interface and the external carbon/glass hybrid laminated reinforcement can be expressed in this method.

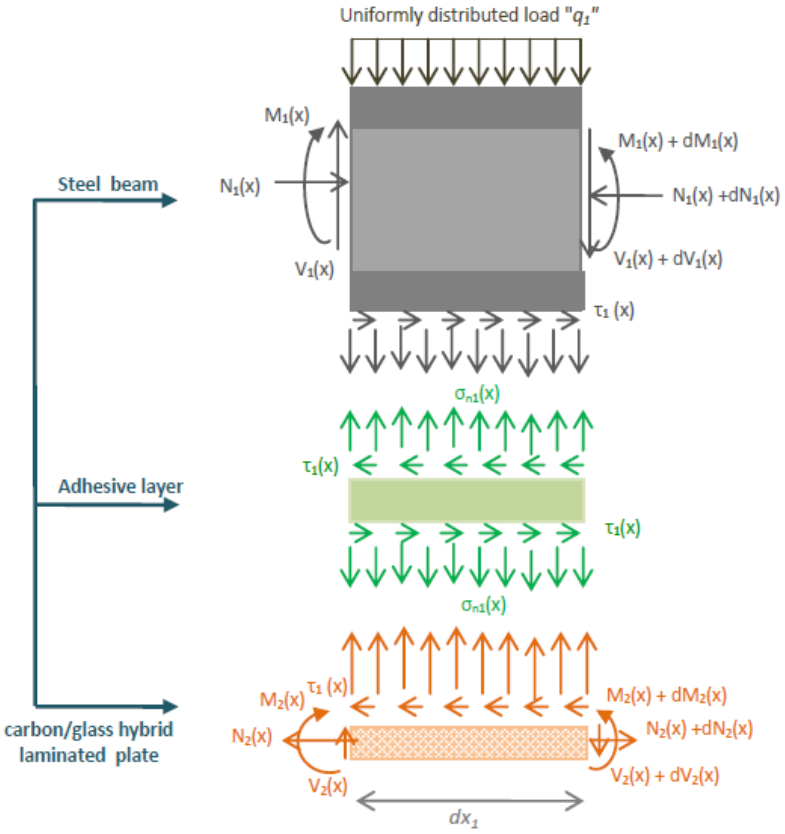

Fig. 3 Forces in infinitesimal element of a steel beam strengthened with prestressed carbon/glass hybrid laminated plate: *Strengthened in Span: lower part*

The governing differential equation for the interfacial shear stress is expressed as (Hassaine Daouadji 2019)

$$\frac{d^2\tau(x)}{dx^2} - \frac{b_2\left[\frac{(y_1+y_2)(y_1+y_2+t_a)}{E_1I_1+E_2I_2}+\frac{1}{E_1A_1}+\frac{1}{E_2A_2}\right]}{\frac{t_a}{G_a}+\frac{t_1}{4G_1}+\frac{5t_2}{12G_2}}\tau(x) + \frac{\left[\frac{y_1+y_2}{E_1I_1+E_2I_2}\right]}{\frac{t_a}{G_a}+\frac{t_1}{4G_1}+\frac{5t_2}{12G_2}}V_{T_{1-2}}(x) = 0 \qquad (22)$$

For simplicity, the general solutions presented below are limited to loading which is either concentrated or uniformly distributed over part or the whole span of the beam, or both. For such loading, $d^2V_T(x)/dx^2=0$, and the general solution to Eq. (22) is given by

$$\tau(x) = \eta_1 \cosh(\xi x) + \eta_2 \sinh(\xi x) + \frac{(t_1+t_2)}{2\xi^2(\frac{t_a}{G_a}+\frac{t_1}{4G_1}+\frac{5t_2}{12G_2})(E_1I_1+E_2I_2)}V_{T1-2}(x) \qquad (23)$$

Where

$$\xi = \left[\frac{b_2\left[\frac{(t_1+t_2)(t_1+t_2+2t_a)}{4(E_1I_1+E_2I_2)}+\frac{1}{E_1A_1}+\frac{1}{E_2A_2}\right]}{\frac{t_a}{G_a}+\frac{t_1}{4G_1}+\frac{5t_2}{12G_2}}\right]^{\frac{1}{2}} \qquad (24)$$

And η_1 and η_2 are constant coefficients determined from the boundary conditions. In the present

study, a simply supported beam has been investigated which is subjected to a uniformly distributed load. For our case of a uniformly distributed load, the formula of the shear stress is given by the following equation

$$\tau(x) = \left[\frac{1}{\xi}\left(\frac{t_a}{G_a} + \frac{t_1}{4G_1} + \frac{5t_2}{12G_2}\right)\left(\frac{A'_{11}}{b_2}P_{0_1} - \frac{y_1 M_{t_{1-2}}(0)}{E_1 I_1}\right)\right] e^{-\xi x} + \frac{(t_1+t_2)\left(a_1 q_1 + x - \frac{e^{-\xi x}}{\xi} q_1\right)}{2\xi^2\left(\frac{t_a}{G_a} + \frac{t_1}{4G_1} + \frac{5t_2}{12G_2}\right)(E_1 I_1 + E_2 I_2)}$$

$$0 \le x \le L_{P_1} \tag{25}$$

2.4 Interfacial shear stress distribution along the carbon/glass hybrid laminated -steel interface "Strengthened in Support: upper part"

A differential section dx, can be cutout from the carbon/glass hybrid laminated composite-strengthened steel, as shown in Fig. 4 "*Strengthened in Support: upper part*". The strains in the continuous steel beam near the adhesive interface and the external carbon/glass hybrid laminated reinforcement can be expressed in this method.

The governing differential equation for the interfacial shear stress is expressed as (Hassaine Daouadji 2019):

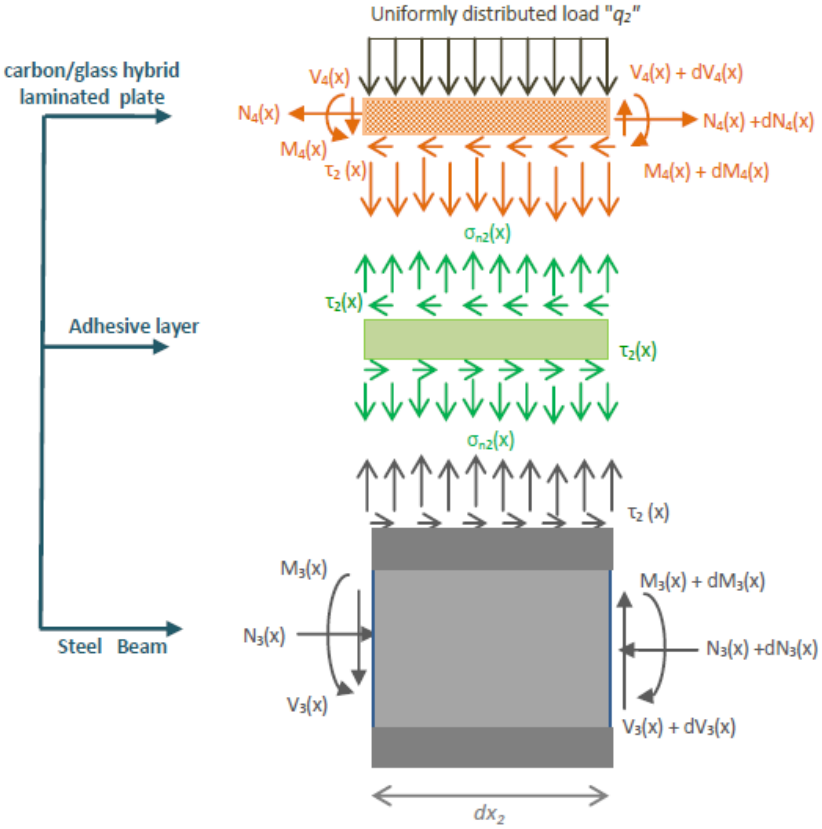

Fig. 4 Forces in infinitesimal element of a steel beam strengthened with prestressed carbon/glass hybrid laminated plate: *Strengthened in Support: upper part*

Allows us to obtain the differential equation of the shear interface stress

$$\frac{d^2\tau(x)}{dx^2}-\frac{G_a}{t_a}\left[A_{11}^{'}+\frac{b_4}{E_3A_3}+\frac{(y_3+\frac{t_4}{2})(y_3+t_a+\frac{t_4}{2})}{E_3I_3D_{11}^{'}+b_4}b_4D_{11}^{'}\right]\tau(x)+\frac{G_a}{t_a}\left[\frac{(y_3+\frac{t_4}{2})}{E_3I_3D_{11}^{'}+b_4}D_{11}^{'}\right]V_{T3-4}(x)=0 \quad (26)$$

The solution to the differential equation (Eq. (26)) above is given by

$$\tau(x)=\eta_3\cos\hbar(\delta x)+\eta_4\sin\hbar(\delta x)+\left[\frac{1}{2\delta^2}(\frac{t_a}{G_a}+\frac{t_3}{4G_3}+\frac{5t_4}{12G_4})(\frac{(2y_3+t_4)}{E_3I_3D_{11}^{'}+b_4}D_{11}^{'})\right]V_{T3-4}(x) \quad (27)$$

With

$$\delta=\left[\frac{A_{11}^{'}+\frac{b_4}{E_3A_3}+\frac{(2y_3+t_4)(2y_3+2t_a+t_4)}{4E_3I_3D_{11}^{'}+b_4}b_4D_{11}^{'}}{\frac{t_a}{G_a}+\frac{t_3}{4G_3}+\frac{5t_4}{12G_4}}\right]^{\frac{1}{2}} \quad (28)$$

And η_3 and η_4 are constant coefficients determined from the boundary conditions. For our case of a uniformly distributed load, the formula of the shear stress is given by the following equation

$$\tau(x)=\eta_4e^{-\delta x}+\left[\frac{1}{2\delta^2}(\frac{t_a}{G_a}+\frac{t_3}{4G_3}+\frac{5t_4}{12G_4})(\frac{(2y_3+t_4)}{E_3I_3D_{11}^{'}+b_4}D_{11}^{'}\right]q_2(a_2+x) \qquad 0\le x\le L_{P2} \quad (29)$$

With

$$\eta_4=\frac{1}{\delta}(\frac{t_a}{G_a}+\frac{t_3}{4G_3}+\frac{5t_4}{12G_4})(\frac{A_{11}^{'}}{b_4}P_{02}-\frac{y_1M_{t_{3-4}}(0)}{E_3I_3})-\left[\frac{1}{2\delta^2}(\frac{t_a}{G_a}+\frac{t_3}{4G_3}+\frac{5t_4}{12G_4})(\frac{(2y_3+t_4)}{E_3I_3D_{11}^{'}+b_4}D_{11}^{'}\right]\frac{q_2}{\delta} \quad (30)$$

3. Numerical results and discussions

As a part of a research project on strengthening existing steel bridges using composite materials a demonstration study was performed on an old railway steel bridge. The aim of this study was to investigate practical difficulties that might be encountered when the strengthening technique is applied to existing structures. In this context we have studied several types of steel structures, among them the one presented in Fig. 5, the characteristics of which are presented on Table 1. It was recognized earlier in this study that if prestressed carbon fiber and/or glass fiber laminates are to be employed for strengthening this steel beam, high shear stresses at the end of the laminates might cause premature debonding failure of the laminates at these locations. One question was whether or not special anchorage device are needed to ensure sufficient anchorage strength. It was also recognized that there is some lack of knowledge regarding how material properties for the carbon/glass hybrid laminated composite materials and the adhesives should be chosen in order to minimize the magnitude of shear stresses at the ends of the laminates without reducing the efficiency of the strengthening technique.

3.1 Material used

The material used for the present studies is an steel beam with variable section bonded by a prestressed with carbon/glass hybrid laminated plate. The steel a beam is subjected to a uniformly distributed load. A summary of the geometric and material properties is given in Table 1 and Fig. 5. The span of the steel continuous beam is (L_{p1}=3500 mm, L_{p2}=2000 mm), the distance from the

Table 1 Geometric and mechanical properties of the materials used

Component	Width (mm)	Depth (mm)	Young's modulus (MPa)	Poisson's ratio
Adhesive layer	b_1=b_3=100	t_a=2	E_a=3000	0.35
Fiber Carbone HR	b_2=b_4=100	t_2=4	E_2=140 000	0.28
Fiber Glass E	b_2=b_4=100	t_2=4	E_2=73 000	0.22

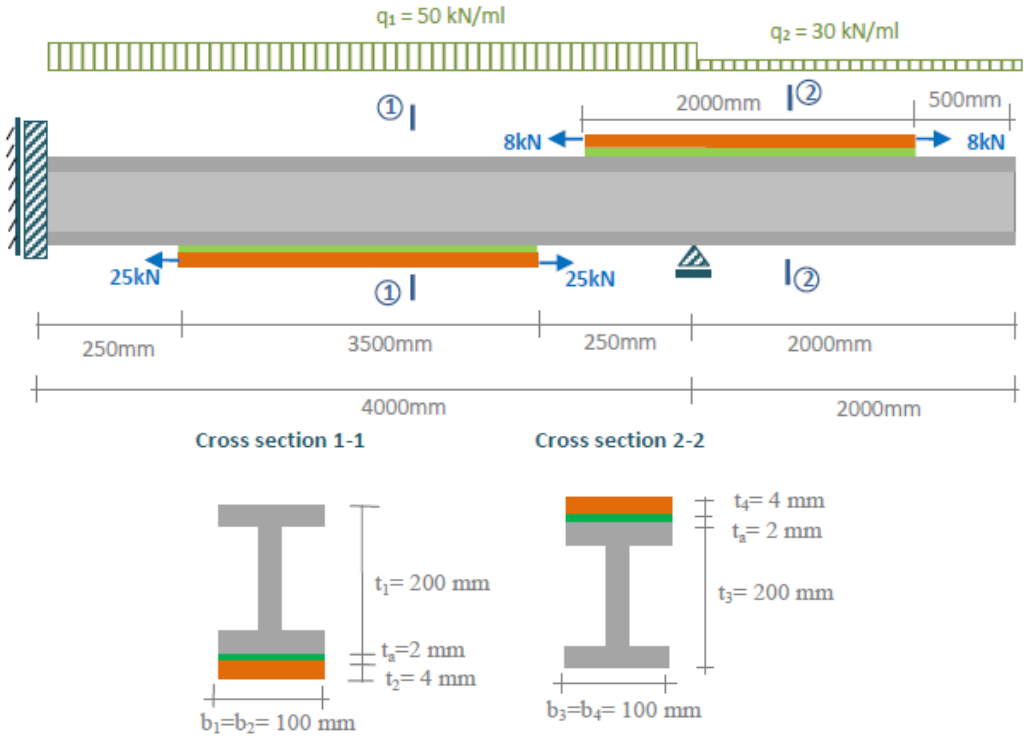

Fig. 5 Geometric characteristic of a steel beam with variable section bonded by a prestressed with carbon/glass hybrid laminated plate

support to the end of the plate is a_1=250 mm and a_2=500 mm and the uniformly distributed load is q_1=50 kN/ml and q_2=30 kN/ml.

3.2 Comparison with analytical solutions

To verify the analytical model, the present predictions are compared firstly with those of Hassaine Daouadji (2019), He (2019) in the case of the absence of the prestressing force and in the second time, a parametric study was presented to show the interest of the prestressing and mechanical characteristics of hybrid composites for strengthening this steel beam. The width of the laminate was kept constant (100 mm) as well as the laminate length which was chosen to L_1=3500 mm and L_2=3500 m leaving a free distance "a_1=250 mm and a_2=500 mm".

The present new solution is compared, in this section, with the closed _ form solution developed by Hassaine Daouadji (2019) and He (2019). This solution does not take into consideration external loads and it is limited to the evaluation of the adhesive shear stress. For the three cases of hybrid

mixture of fibers; namely the first plate in 100% CFRP; second plate of 50% CFRP and 50% GFRP; the third plate in 100% GFRP. Fig. 6 shows an almost exact agreement between the present results and those obtained by the method developed by Hassaine Daouadji (2019) in Span Area and He (2019) in Cantilevered Area. Overall, the interfacial stresses predicted by the present method almost agree with those of Hassaine Daouadji (2019), He (2019) without taking into account the prestressing force (P_o=0), except near the free edge, where the present theory predicts lower values. Hence, it is apparent that the adherend shear deformation reduces the interfacial stresses concentration and thus renders the adhesive shear distribution more uniform.

3.3 Parametric study: Analysis and study of interfacial shear stresses for different parameters

In this section, numerical results of the present solution are presented to study the effect of various parameters on the distributions of the interfacial shear stresses in an steel beam strengthened with carbon/glass hybrid laminated plate. These results are intended to demonstrate the main characteristics of interfacial shear stress distributions in these strengthened beams. The numerical results are presented in Figs. 7-19. The example of the steel beam strengthened with carbon/glass hybrid laminated plate has a span of 4000 mm and 2000 mm in cantilever and the cross-sectional; are presented in Fig. 5.

3.3.1 Effect of the mixture carbon / glass fibers hybrid laminated plate on the interfacial shear stress

Figs. 7 and 8 gives the effect of the mixture carbon/glass fibers hybrid laminated plate (in other words: Effect of hybrid laminated plate stiffness) on interfacial shear stresses in span area and cantilevered area for a steel beam strengthened with prestressed carbon/glass hybrid laminated plate, in order to study this parameter; it is important to treat five variants of the mixture carbon/glass hybrid laminated plate, namely: 100% CFRP and 00% GFRP; 75% CFRP and 25% GFRP; 50% CFRP and 50% GFRP; 25% CFRP and 75% GFRP and 00% CFRP and 100% GFRP respectively, and for two types of prestressing change, the first of which is without prestressing (P_0=0) and in the

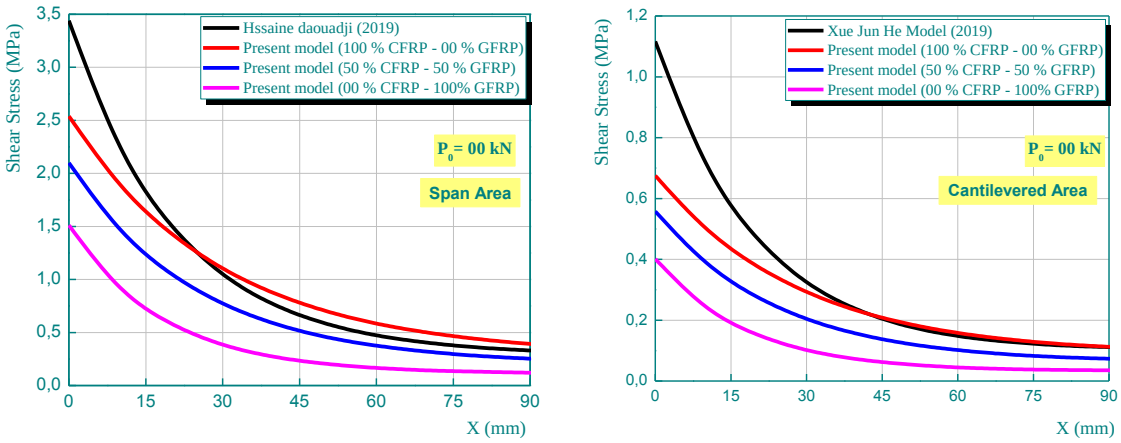

Fig. 6 Comparison of interfacial shear stresses in steel beam strengthened with carbon/glass hybrid laminated plate by the analytical results

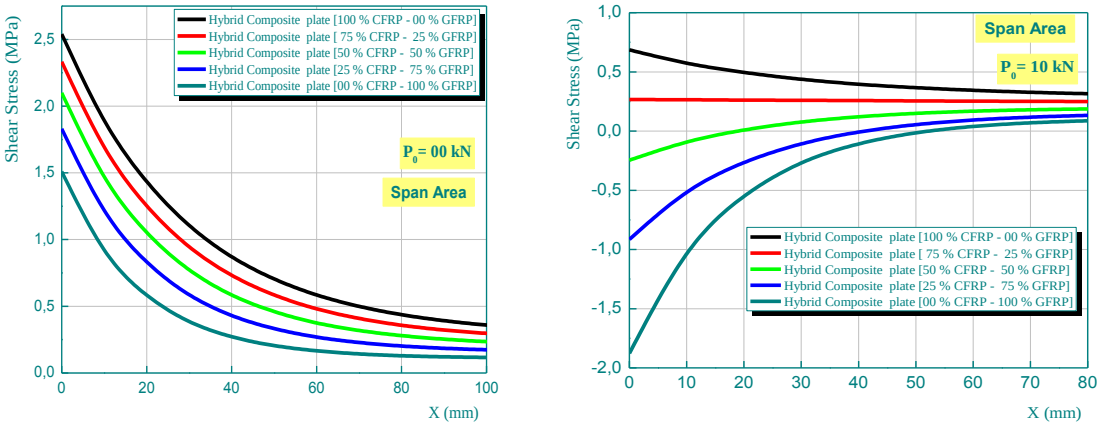

Fig. 7 Effect of plate stiffness on interfacial shear stresses in Span Area for a steel beam strengthened with prestressed carbon/glass hybrid laminated plate

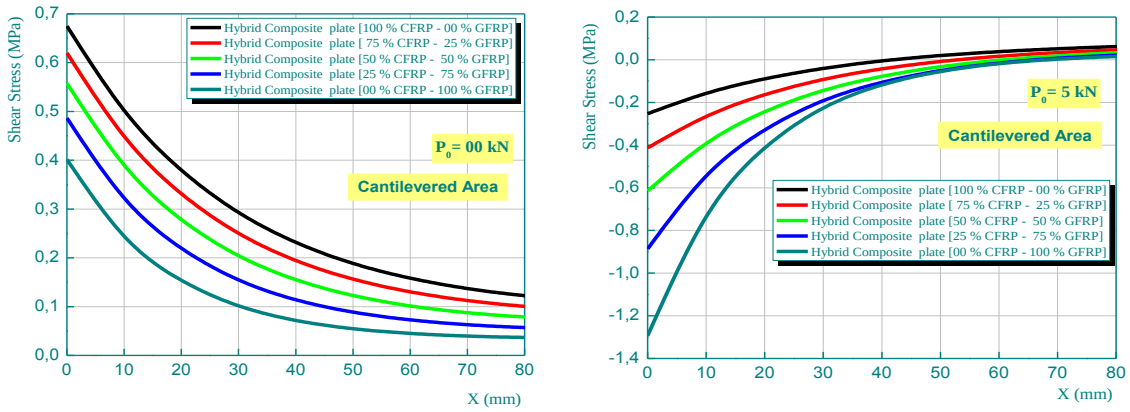

Fig. 8 Effect of plate stiffness on interfacial shear stresses in Cantilevered Area for a steel beam strengthened with prestressed carbon/glass hybrid laminated plate

second type holds the prestressing (P_0=10 kN in Span Area and P_0=5 kN in cantilevered Area). Which demonstrates the effect of plate material properties on interfacial shear stresses. The length of the hybrid laminated plate is L_{p1}=3500 mm and L_{p2}=2000 mm, and the thickness of the plate and the adhesive layer are both 4mm. The results show that, as the plate material becomes softer (from 100% CFRP to 0% CFRP and 50% GFRP and then 100% GFRP), the interfacial shear stresses become smaller, as expected. This is because, under the same load, the tensile force developed in the hybrid laminated plate is which contains more glass fiber (100% GFRP) and less carbon fiber (00% CFRP), which leads to reduced interfacial stresses. The position of the peak interfacial shear stress moves closer to the free edge as the plate becomes less stiff.

3.3.2 Effect of variation of the prestressing force (P_0) of carbon/glass fibers hybrid laminated plate on interfacial shear stress

In this section, numerical results of the present solution are presented to study the effect of the prestressing force P_0 on the distribution of interfacial shear stress in steel beam strengthened with

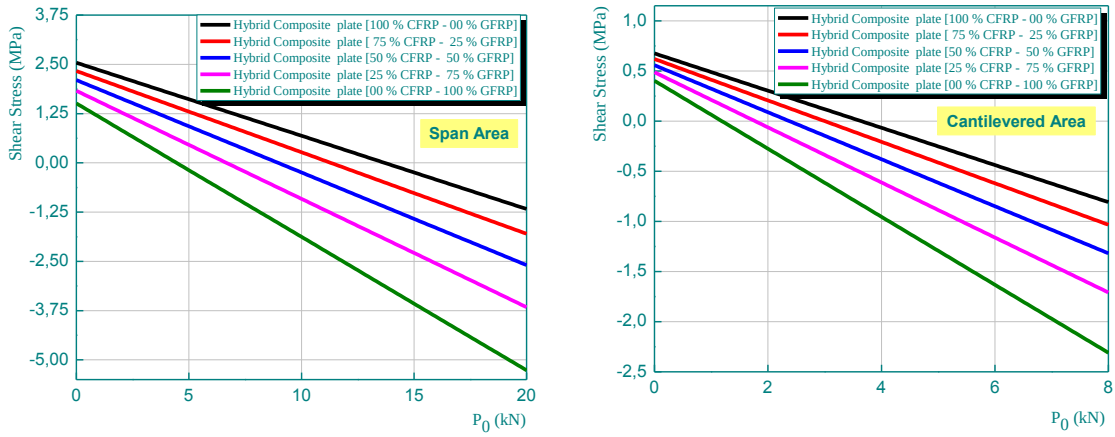

Fig. 9 Effect of the prestressing force on interfacial shear stresses in steel beam strengthened with prestressed carbon/glass hybrid laminated plate

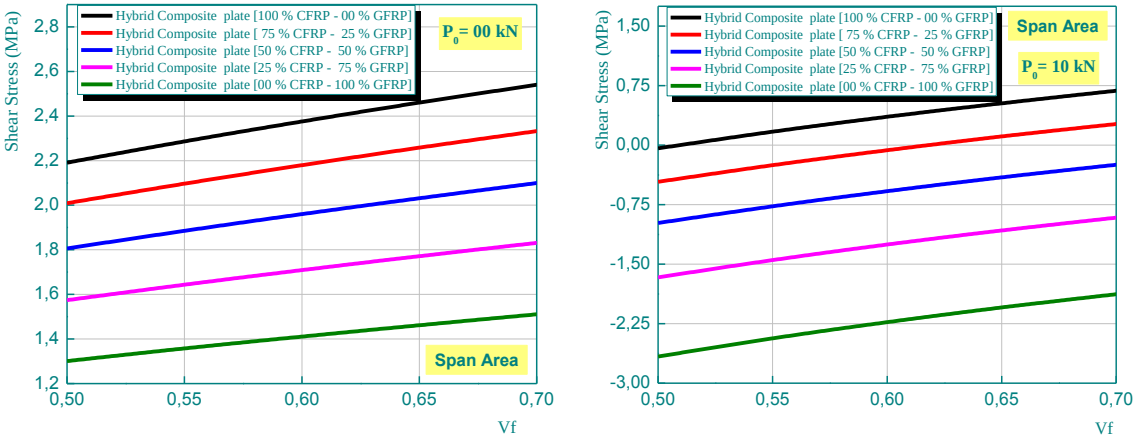

Fig. 10 Effect Fiber volume fractions effect on interfacial shear stresses in Span Area for a steel beam strengthened with prestressed carbon/glass hybrid laminated plate

prestressed carbon/glass hybrid laminated plate. For a different value of the prestressing force P_0 in the span and on the support, as shown in Fig. 9, thus five variants of the mixture carbon/glass hybrid laminated plate, namely: 100% CFRP and 00% GFRP; 75% CFRP and 25% GFRP; 50% CFRP and 50% GFRP; 25% CFRP and 75% GFRP and 00% CFRP and 100% GFRP.

Fig. 9 plot the interfacial shear and normal stress for the steel beam strengthened with prestressed carbon/glass hybrid laminated plate. From these results, one can notice that the maximum shear stress occur at the ends of adhesively bonded plates, or peeling, stress disappears at around 18 mm from the end of the plates. And, it is seen that increasing the value of prestressing force p_0 leads to high shear stress concentrations.

3.3.3 Fiber volume fractions effect of carbon / glass hybrid laminated plate on interfacial shear stress

Figs. 10 and 11 shows, the effect of fiber volume fractions V_f(=0.5, 0.55, 0.6, 0.65 and 0.7) on

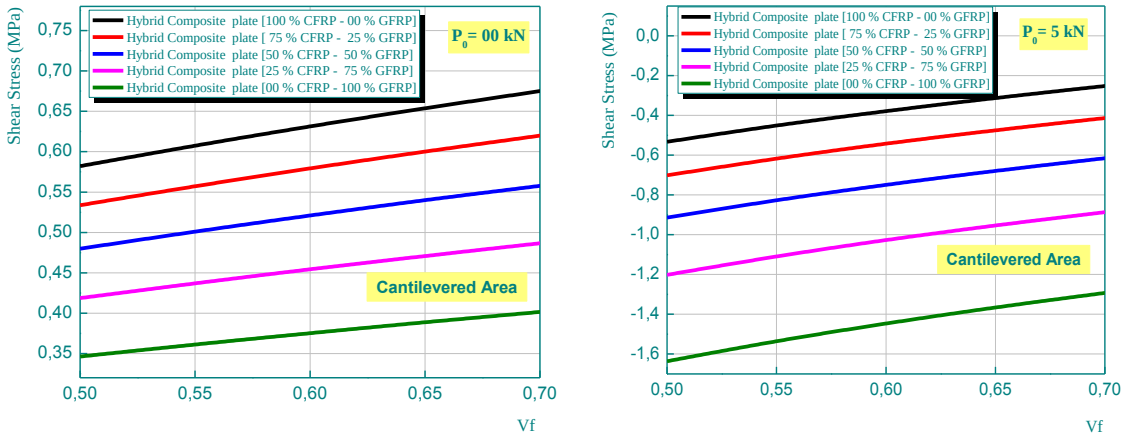

Fig. 11 Effect Fiber volume fractions effect on interfacial shear stresses in Cantilevered Area for a steel beam strengthened with prestressed carbon/glass hybrid laminated plate

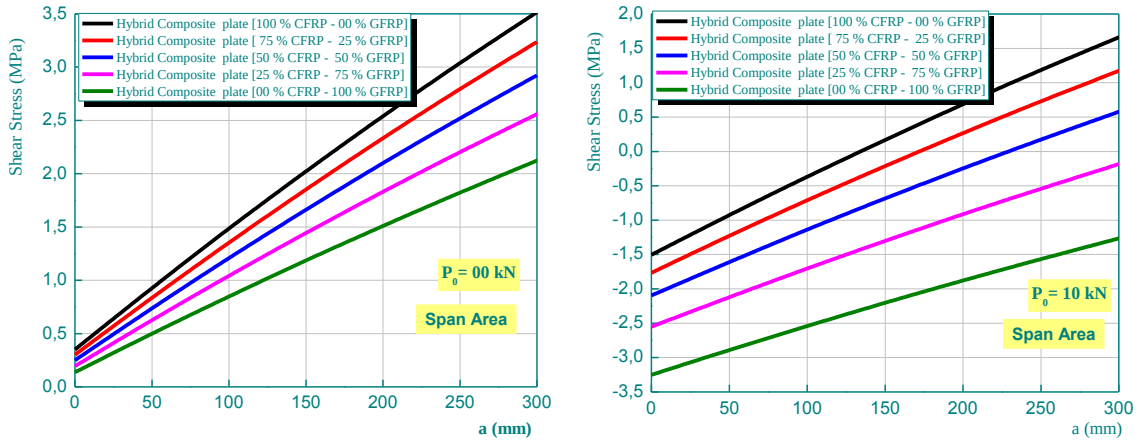

Fig. 12 Effect of plate length of the strengthened L_p on interfacial shear stresses in Span Area for a steel beam strengthened with prestressed carbon/glass hybrid laminated plate

the variation of shear adhesive stresses in span area and cantilevered area for a steel beam strengthened with prestressed carbon/glass hybrid laminated plate. For the five values of fiber volume fractions V_f (=0.5, 0.55, 0.6, 0.65 and 0.7) of the hybrid laminated in the span and on the support, as shown in Figs. 10 and 11, In that case five variants of the mixture carbon/glass hybrid laminated plate, namely: 100% CFRP and 00% GFRP; 75% CFRP and 25% GFRP; 50% CFRP and 50% GFRP; 25% CFRP and 75% GFRP and 00% CFRP and 100% GFRP. And of course for two types of prestressing change, the first of which is without prestressing (P_0=0) and in the second type holds the prestressing (P_0=10 kN in span area and P_0=5 kN in cantilevered area). It can be seen that the interfacial shear stresses are reduced with decreases in fiber volume fraction. However, almost no effect is observed on the variation of interfacial normal stresses.

3.3.4 Effect on plate length of the strengthened steel beam region L_p

The influence of the length of the ordinary-steel beam region (the region between the support

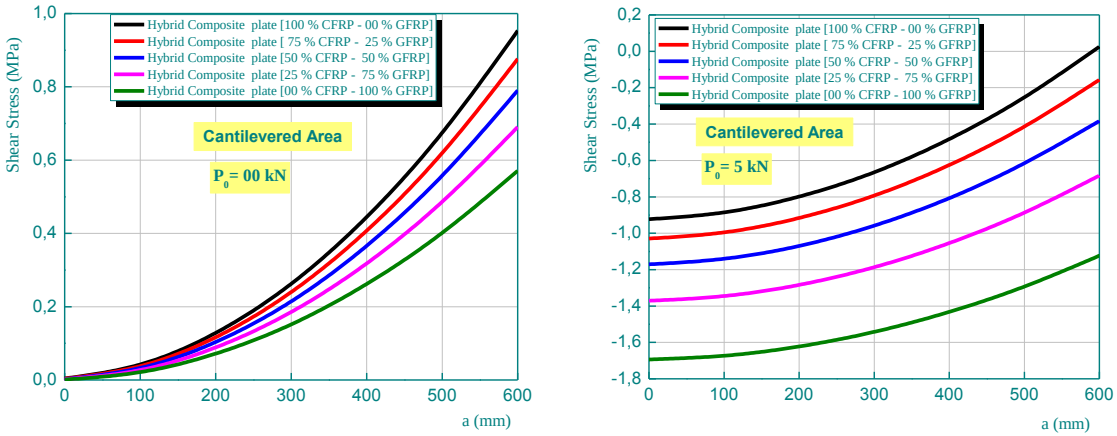

Fig. 13 Effect of plate length of the strengthened L_p on interfacial shear stresses in Cantilevered Area for a steel beam strengthened with prestressed carbon/glass hybrid laminated plate

and the end of the hybrid laminated plate strip on the edge stresses) on interfacial shear stresses in span area and cantilevered area for a steel beam strengthened with prestressed carbon/glass hybrid laminated plate; appears in Figs. 12 and 13. For the study of this length "L_P", we have used the five variants of the mixture carbon / glass hybrid laminated plate, namely: 100% CFRP and 00% GFRP; 75% CFRP and 25% GFRP; 50% CFRP and 50% GFRP; 25% CFRP and 75% GFRP and 00% CFRP and 100% GFRP respectively, and for two types of prestressing change, the first of which is without prestressing (P_0=0 kN) and in the second type holds the prestressing (P_0=10 kN in span area and P_0=5 kN in cantilevered area). Which demonstrates the effect of plate material properties on interfacial shear stresses. It is seen that, as the hybrid laminated plate terminates further away from the supports, the interfacial stresses increase significantly. This result reveals that in any case of strengthening, including cases where retrofitting is required in a limited zone of maximum bending moments, it is recommended to extend the strengthening strip as possible to the lines.

3.3.5 Effect of plate thickness of carbon/glass fibers hybrid laminated plate on interfacial shear stress

The thickness of the carbon/glass hybrid laminated plate is an important design variable in practice. Figs. 14 and 15 shows the effect of the thickness of the carbon/glass hybrid laminated plate on the interfacial shear stresses. For a different value of the thickness of the hybrid laminated in the span and on the support, as shown in Figs. 14 and 15, In that case five variants of the mixture carbon/glass hybrid laminated plate, namely: 100% CFRP and 00% GFRP; 75% CFRP and 25% GFRP; 50% CFRP and 50% GFRP; 25% CFRP and 75% GFRP and 00% CFRP and 100% GFRP.

It is shown that the level and concentration of interfacial shear stress are influenced considerably by the thickness of the carbon/glass hybrid laminated plate. The interfacial shear stresses increase as the thickness of prestressed carbon/glass hybrid laminated plate increases and for the different variants of the mixture carbon/glass hybrid laminated. Generally, the thickness of hybrid laminated plates used in practical engineering is small, compared with that of steel plate or other thick material plate. Therefore, the fact of the smaller interfacial shear stress level and concentration should be one of the advantages of retrofitting by prestressed carbon/glass hybrid laminated plate compared with a thick material plate.

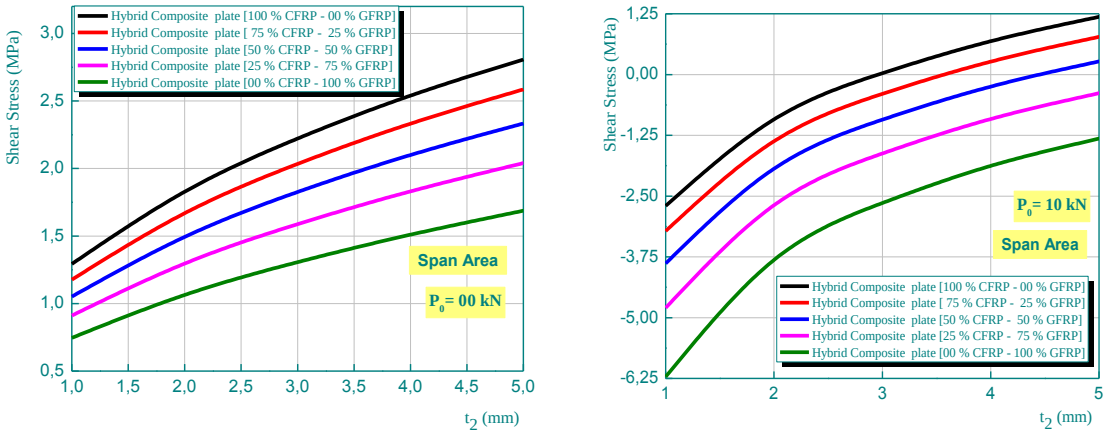

Fig. 14 Effect of plate thickness on interfacial shear stresses in Span Area for a steel beam strengthened with prestressed carbon/glass hybrid laminated plate

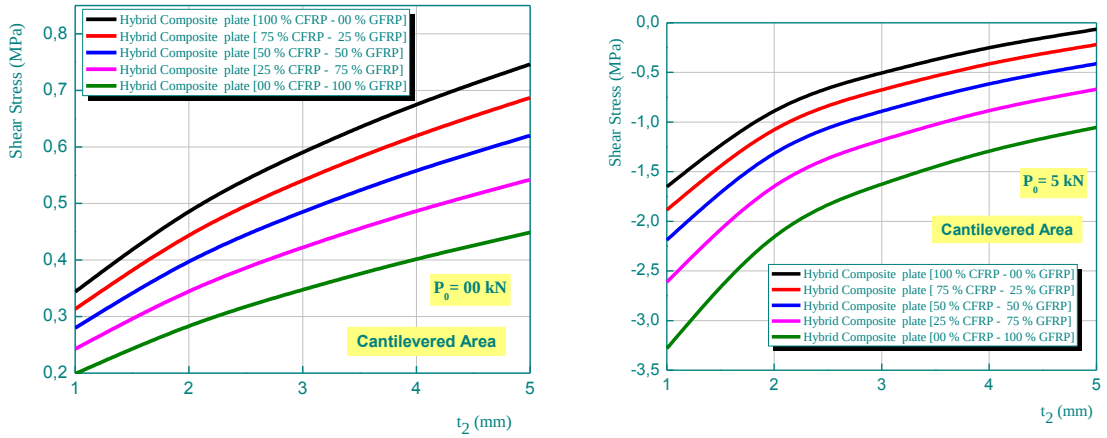

Fig. 15 Effect of plate thickness on interfacial shear stresses in Cantilevered Area for a steel beam strengthened with prestressed carbon/glass hybrid laminated plate

3.3.6 Effect of the adhesive layer thickness

Figs. 16 and 17 shows the effect of the thickness of the adhesive layer on interfacial shear stress of shear adhesive stresses in span area and cantilevered area for a steel beam strengthened with prestressed carbon/glass hybrid laminated plate. Taking into account as previously the different proportions of the mixture in CFRP and GFRP as well as the effect of the prestressing as shown in Figs. 16 and 17. It is seen that increasing the thickness of the adhesive layer leads to significant reduction in peak interfacial shear stress. Thus using thick adhesive layer, especially in the vicinity of the edge, is recommended.

3.3.7 Effect of elasticity modulus of adhesive layer

The adhesive layer is a relatively soft, isotropic material and has a smaller stiffness. The four sets of Young's moduli are considered here, which are 3, 4, 5 and 6.5 GPa. The Poisson's ratio of the adhesive is kept constant. As shown in Figs. 16 and 17, the effect of elasticity modulus of

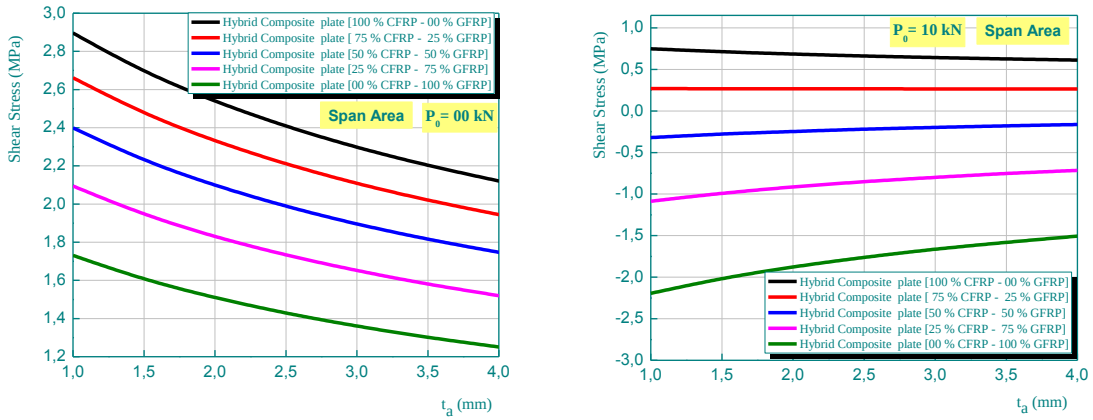

Fig. 16 Effect of the adhesive layer thickness on interfacial shear stresses in Span Area for a steel beam strengthened with prestressed carbon/glass hybrid laminated plate

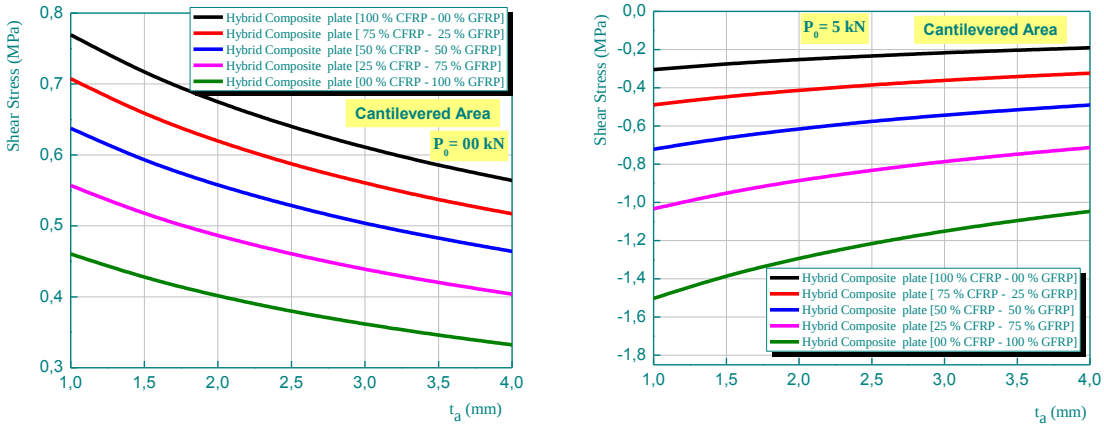

Fig. 17 Effect of the adhesive layer thickness on interfacial shear stresses in Cantilevered Area for a steel beam strengthened with prestressed carbon/glass hybrid laminated plate

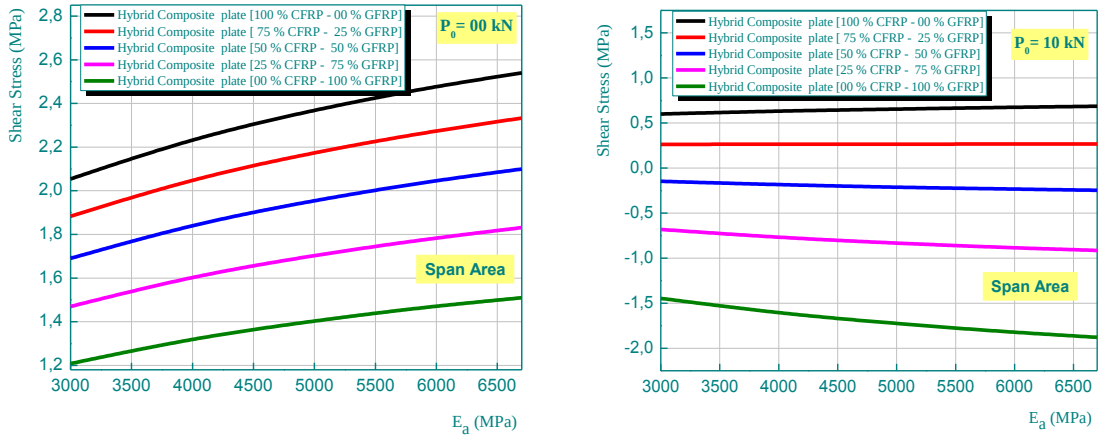

Fig. 18 Effect of elasticity modulus of adhesive layer on interfacial shear stresses in Span Area for a steel beam strengthened with prestressed carbon/glass hybrid laminated plate

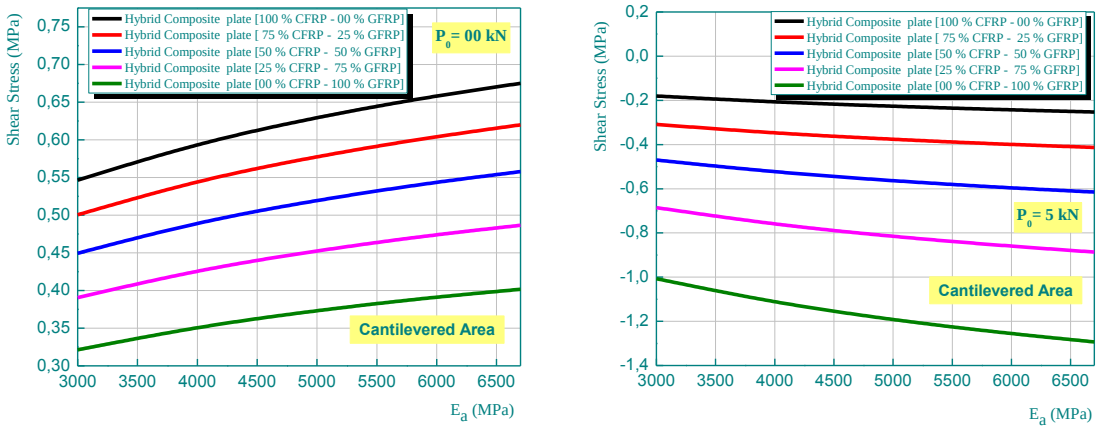

Fig. 19 Effect of elasticity modulus of adhesive on interfacial shear stresses in Cantilevered Area for a steel beam strengthened with prestressed carbon/glass hybrid laminated plate

adhesive layer on interfacial shear stress of shear adhesive stresses in span area and cantilevered area for a steel beam strengthened with prestressed carbon/glass hybrid laminated plate. The numerical results in Figs. 18 and 19 show that the property of the adhesive hardly influences the level of the interfacial shear stresses, whether shear stress, but the stress concentrations at the end of the plate increase as the Young's modulus of the adhesive increases.

4. Conclusions

In the present study, a new theoretical interfacial shear stresses in span area in cantilevered area for a steel beam strengthened with prestressed carbon/glass hybrid laminated plate, analysis has been presented and which will be the object of a realization to an existing steel structural strengthened with bonded prestressed hybrid laminates. This type of reinforcement has clearly shown its effectiveness, since there will be the possibility of using plates either rigid (case of CFRP) or flexible (case of GFRP) and the best solutions recommended by manufacturers is the hybrid plate "neither flexible nor rigid (case of this present carbon/glass hybrid laminated plate)". The theoretical predictions are compared with other existing solutions, the present model is general in nature, and it is applicable to more general loads cases. The results show that there exists a high concentration of shear and peeling stress at the ends of the prestressed carbon/glass hybrid laminates. The effective modulus of the externally prestressed bonded hybrid FRP plate increases with an increasing percentage of Fiber volume fractions of carbon/glass hybrid laminated. It is found that laminates with higher E-modulus, produce a lower concentration of interfacial shear stress at the ends of the laminate. The shear modulus of the adhesive material was found to have a substantial effect on the magnitude of maximum interfacial stress at the end of the laminate. Using more flexible adhesives results in a more uniform distribution of interfacial shear stress and reduces the value of maximum critical interfacial stress at the ends of the laminate.

The parametric study has also shown that in practical applications, where prestressed carbon/glass hybrid laminated plates are to be used for strengthening structural members, mechanical anchorage devices should be employed in order to avoid premature failure of the

strengthening scheme and ensure sufficient anchorage capacity at the ends of the laminates. The results show that the prestressing has a significant effect on the interfacial shear stresses in steel beam strengthened with prestressed carbon/glass hybrid laminated plate, especially, when the length of the reinforcement is equal to the length of the steel beam. Consequently, il est recommandé d'étendre au maximum la bande de renforcement jusqu'aux lignes (supports). It is seen that, as the hybrid laminated plate terminates further away from the supports, the interfacial stresses increase significantly. This research is helpful for the understanding on mechanical behaviour of the interface and design of the FRP-steel hybrid structures.

Acknowledgments

This research was supported by the Algerian Ministry of Higher Education and Scientific Research (MESRS) as part of the grant for the PRFU research project n° A01L02UN140120200002 and by the University of Tiaret, in Algeria.

References

Abderezak, R., Daouadji, T.H. and Rabia, B. (2021b), "Aluminum beam reinforced by externally bonded composite materials", *Adv. Mater. Res.*, **10**(1), 23-44. http://doi.org/10.12989/amr.2021.10.1.023.

Abderezak, R., Rabia, B., Daouadji, T.H., Abbes, B., Belkacem, A. and Abbes, F. (2019), "Elastic analysis of interfacial stresses in prestressed PFGM-RC hybrid beams", *Adv. Mater. Res.*, **7**(2), 83-103. https://doi.org/10.12989/amr.2018.7.2.083.

Akbas Seref D. (2018), "Thermal post-buckling analysis of a laminated composite beam", *Struct. Eng. Mech.*, **67**(4), 337-34. http://doi.org/10.12989/sem.2018.67.4.337.

Al-Furjan, M.S.., Habibi, M., Ghabussi, A., Safarpour, H., Safarpour, M. and Tounsi, A. (2021), "Non-polynomial framework for stress and strain response of the FG-GPLRC disk using three-dimensional refined higher-order theory", *Eng. Struct.*, **228**(1), 111496. https://doi.org/10.1016/j.engstruct.2020.111496.

Amara, K., Antar, K. and Benyoucef, S. (2019), "Hygrothermal effects on the behavior of reinforced-concrete beams strengthened by bonded composite laminate plates", *Struct. Eng. Mech.*, **69**(3), 327-334. https://doi.org/10.12989/sem.2019.69.3.327.

Ameur, M., Tounsi, A., Benyoucef, S., Bouiadjra, M.B. and Bedia, E.A. (2008), "Stress analysis of steel beams strengthened with a bonded hygrothermal aged composite plate", *Int. J. Mech. Mater. Des.*, **5**(2), 143-156. https://doi.org/10.1007/s10999-008-9090-2.

Benachour, A., Benyoucef, S., Tounsi, A. and Adda Bedia, E.A. (2008), "Interfacial stress analysis of steel beams reinforced with bonded prestressed FRP plate", *Eng. Struct*., **30**, 3305-3315. https://doi.org/10.1016/j.engstruct.2008.05.007.

Benferhat, R., Hassaine Daouadji, T. and Abderezak, R. (2020a), "Thermo-mechanical behavior of porous FG plate resting on the Winkler-Pasternak foundation", *Coupl. Syst. Mech.*, **9**(6), 499-519. http://doi.org/10.12989/csm.2020.9.6.499.

Benferhat, R., Hassaine Daouadji, T. and Rabahi, A. (2020b),"Predictions of the maximum plate end stresses of imperfect FRP strengthened RC beams: study and analysis", *Adv. Mater. Res.*, **9**(4), 265-287. http://doi.org/10.12989/amr.2020.9.4.265.

Benferhat, R., Hassaine Daouadji, T. and Rabahi, A. (2021c), "Analysis and sizing of RC beams reinforced by external bonding of imperfect functionally graded plate", *Adv. Mater. Res.*, **10**(2), 77-98. http://doi.org/10.12989/amr.2021.10.2.077.

Bensattalah, T., Daouadji, T.H. and Zidour, M. (2020b), "Influences the shape of the floor on the behavior of buildings under seismic effect", *Proceedings of the 4th International Symposium on Materials and*

Sustainable Development, Vol1-Nano Technology and Advanced Materials, 26-42. https://doi.org/10.1007/978-3-030-43268-3_3.

Bouakaz, K., Daouadji, T.H., Meftah, S.A., Ameur, M., Tounsi, A. and Bedia, E.A. (2014), "A numerical analysis of steel beams strengthened with composite materials", *Mech. Compos. Mater.*, **50**(4), 685-696. https://doi.org/10.1007/s11029-014-9435-x.

Chedad, A., Daouadji, T.H., Abderezak, R., Belkacem, A., Abbes, B., Rabia, B. and Abbes, F. (2018), "A high-order closed-form solution for interfacial stresses in externally sandwich FGM plated RC beams", *Adv. Mater. Res.*, **6**(4), 317-328. https://doi.org/10.12989/amr.2017.6.4.317.

Chergui, S., Daouadji, T.H., Hamrat, M., Boulekbache, B., Bougara, A., Abbes, B. and Amziane, S. (2019), "Interfacial stresses in damaged RC beams strengthened by externally bonded prestressed GFRP laminate plate: Analytical and numerical study", *Adv. Mater. Res.*, **8**(3), 197-217. https://doi.org/10.12989/amr.2019.8.3.197.

Das, O., Ozturk, H. and Gonenli, C. (2020), "Finite element vibration analysis of laminated composite parabolic thick plate frames", *Steel Compos. Struct.*, **35**(1), 43-59. http://doi.org/10.12989/scs.2020.35.1.043.

David, H., Rodrigo, G., Carlos, S. and Dinar, C. (2020), "GBT-based time-dependent analysis of steel-concrete composite beams including shear lag and concrete cracking effects", *Thin Wall. Struct.*, **150**, 106706. https://doi.org/10.1016/j.tws.2020.106706.

enferhat, R., Daouadji, T.H. and Abderezak, R. (2021a), "Effect of porosity on fundamental frequencies of FGM sandwich plates", *Compos. Mater. Eng.*, **3**(1), 25-40. http://doi.org/10.12989/cme.2021.3.1.025.

Hadj, B., Rabia, B. and Daouadji, T.H. (2021), "Vibration analysis of porous FGM plate resting on elastic foundations: Effect of the distribution shape of porosity", *Coupl. Syst. Mech.*, **10**(1), 61-77. http://doi.org/10.12989/csm.2021.10.1.061.

Hamrat, M., Bouziadi, F., Boulekbache, B., Daouadji, T.., Chergui, S., Labed, A. and Amziane, S. (2020), "Experimental and numerical investigation on the deflection behavior of pre-cracked and repaired reinforced concrete beams with fiber-reinforced polymer", *Constr. Build. Mater.*, **249**, 118745. http://doi.org/10.1016/j.conbuildmat.2020.118745.

Hassaine Daouadji, T. (2013), "Analytical analysis of the interfacial stress in damaged reinforced concrete beams strengthened by bonded composite plates", *Strength Mater.*, **45**(5), 587-597. https://doi.org/10.1007/s11223-013-9496-4.

Hassaine Daouadji, T. (2017), "Analytical and numerical modeling of interfacial stresses in beams bonded with a thin plate", *Adv. Comput. Des.*, **2**(1), 57-69. https://doi.org/10.12989/acd.2017.2.1.057

Hassaine Daouadji, T., Bensattalah, T., Rabahi, A. and Tounsi, A. (2021a), "New approach of composite wooden beam- reinforced concrete slab strengthened by external bonding of prestressed composite plate: Analysis and modeling", *Struct. Eng. Mech.*, **78**(3), 319-332. http://doi.org/10.12989/sem.2021.78.3.31.

Hassaine Daouadji, T., Rabahi, A. and Benferhat, R. (2020), "Flexural performance of wooden beams strengthened by composite plate", *Struct. Monit. Mainten.*, **7**(3), 233-259. http://doi.org/10.12989/smm.2020.7.3.233.

Hassaine Daouadji, T., Rabahi, A., Benferhat, R. and Adim, B. (2019), "Flexural behaviour of steel beams reinforced by carbon fibre reinforced polymer: Experimental and numerical study", *Struct. Eng. Mech.*, **72**(4), 409-419. https://doi.org/10.12989/sem.2019.72.4.409.

Hassaine Daouadji, T., Rabahi, A., Benferhat, R. and Tounsi, A. (2021b), "Performance of damaged RC continuous beams strengthened by prestressed laminates plate: Impact of mechanical and thermal properties on interfacial stresses", *Coupl. Syst. Mech.*, **10**(2), 161-184. http://doi.org/10.12989/csm.2021.10.2.161.

Hassaine Daouadji, T., Rabahi, A., Benferhat, R. and Tounsi, A. (2021c), "Impact of thermal effects in FRP-RC hybrid cantilever beams", *Struct. Eng. Mech.*, **78**(5), 573-583. http://doi.org/10.12989/sem.2021.78.5.573.

He, X.J., Zhou, C.Y. and Wang, Y. (2019), "Interfacial stresses in reinforced concrete cantilever members strengthened with fibre-reinforced polymer laminates", *Adv. Struct. Eng.*, **23**(2), 277-288. https://doi.org/10.1177/1369433219868933.

Henni, M.A.B., Abbes, B., Daouadji, T.H., Abbes, F. and Adim, B. (2021), "Numerical modeling of

hygrothermal effect on the dynamic behavior of hybrid composite plates", *Steel Compos. Struct.*, **39**(6), 751-763. http://doi.org/10.12989/scs.2021.39.6.751.

Kablia, A., Benferhat, R., Hassaine Daouadji, T. and Bouzidene, A. (2020), "Effect of porosity distribution rate for bending analysis of imperfect FGM plates resting on Winkler-Pasternak foundations under various boundary conditions", *Coupl. Syst. Mech.*, **9**(6), 575-597. http://doi.org/10.12989/csm.2020.9.6.575.

Krour, B., Bernard, F. and Tounsi, A. (2014), "Fibers orientation optimization for concrete beam strengthened with a CFRP bonded plate: A coupled analytical-numerical investigation", *Eng. Struct.*, **56**, 218-227. https://doi.org/10.1016/j.engstruct.2013.05.008.

Liu, S., Zhou, Y., Zheng, Q., Zhou, J., Jin, F. and Fan, H. (2019), "Blast responses of concrete beams reinforced with steel-GFRP composite bars", *Struct.*, **22**, 200-212. https://doi.org/10.1016/j.istruc.2019.08.010.

Mercan, K., Ebrahimi, F. and Civalek, O. (2020), "Vibration of angle-ply laminated composite circular and annular plates", *Steel Compos. Struct.*, **34**(1), 141-154. http://doi.org/10.12989/scs.2020.34.1.141.

Panjehpour, M., Ali, A.A.A., Voo, Y.L. and Aznieta, F.N. (2014), "Effective compressive strength of strut in CFRP-strengthened reinforced concrete deep beams following ACI 318-11", *Comput. Concrete*, **13**(1), 135-165. https://doi.org/10.12989/cac.2014.13.1.135.

Panjehpour, M., Farzadnia, N., Demirboga, R. and Ali, A.A.A. (2016), "Behavior of high-strength concrete cylinders repaired with CFRP sheets", *J. Civil Eng. Manage.*, **22**(1), 56-64. https://doi.org/10.3846/13923730.2014.897965.

Rabahi, A., Hassaine Daouadji, T. and Benferhat, R. (2020), "Analysis of interfacial stresses of the reinforced concrete foundation beams repairing with composite materials plate", *Coupl. Syst. Mech.*, **9**(5), 473-498. http://doi.org/10.12989/csm.2020.9.5.473.

Rabahi, A., Hassaine Daouadji, T. and Benferhat, R. (2021a), "Modeling and analysis of the imperfect FGM-damaged RC hybrid beams", *Adv. Comput. Des.*, **6**(2), 117-133. http://doi.org/10.12989/acd.2021.6.2.117.

Rabahi, A., Hassaine Daouadji, T., Benferhat, R. and Tounsi, A. (2021c), "Mechanical behavior of RC cantilever beams strengthened with FRP laminate plate", *Adv. Comput. Des.*, **6**(3), 169-190. http://doi.org/10.12989/acd.2021.6.3.169.

Rabahi, A., Hassaine Daouadji, T., Benferhat, R. and Tounsi, A. (2021d), "New proposal for flexural strengthening of a continuous I-steel beam using FRP laminate under thermo-mechanical loading", *Struct. Eng. Mech.*, **78**(6), 703-714. http://doi.org/10.12989/sem.2021.78.6.703.

Rabia, B., Daouadji, T.H. and Abderezak, R. (2019), "Effect of porosity in interfacial stress analysis of perfect FGM beams reinforced with a porous functionally graded materials plate", *Struct. Eng. Mech.*, **72**(3), 293-304. https://doi.org/10.12989/sem.2019.72.3.293.

Rabia, B., Daouadji, T.H. and Abderezak, R. (2021b), "Effect of air bubbles in concrete on the mechanical behavior of RC beams strengthened in flexion by externally bonded FRP plates under uniformly distributed loading", *Compos. Mater. Eng.*, **3**(1), 41-55. http://doi.org/10.12989/cme.2021.3.1.041.

Safaei, B. (2020), "The effect of embedding a porous core on the free vibration behavior of laminated composite plates", *Steel Compos. Struct.*, **35**(5), 659-670. http://doi.org/10.12989/scs.2020.35.5.659.

Smith, S.T. and Teng, J.G. (2002), "Interfacial stresses in plated beams", *Eng. Struct.*, **23**(7), 857-871. http://doi.org/10.1016/S0141-0296(00)00090-0.

Tayeb, B. and Daouadji, T.H (2020a), "Improved analytical solution for slip and interfacial stress in composite steel-concrete beam bonded with an adhesive", *Adv. Mater. Res.*, **9**(2), 133-153. https://doi.org/10.12989/amr.2020.9.2.133.

Tlidji, Y., Benferhat, R. and Tahar, H.D. (2021), "Study and analysis of the free vibration for FGM microbeam containing various distribution shape of porosity", *Struct. Eng. Mech.*, **77**(2), 217-229. http://doi.org/10.12989/sem.2021.77.2.217.

Tounsi, A. (2006), "Improved theoretical solution for interfacial stresses in concrete beams strengthened with FRP plate", *Int. J. Solid. Struct.*, **43**(14-15), 4154-4174. https://doi.org/10.1016/j.ijsolstr.2005.03.074.

Tounsi, A., Daouadji, T.H. and Benyoucef, S. (2008), "Interfacial stresses in FRP-plated RC beams: Effect of adherend shear deformations", *Int. J. Adhes. Adhesiv.*, **29**(4), 343-351. https://doi.org/10.1016/j.ijadhadh.2008.06.008.

Zohra, A., Benferhat, R., Tahar, H.D. and Tounsi, A. (2021), "Analysis on the buckling of imperfect

functionally graded sandwich plates using new modified power-law formulations", *Struct. Eng. Mech.*, **77**(6), 797-807. http://doi.org/10.12989/sem.2021.77.6.797.

AI